Supporting Information

Melanin-like nanofibers with highly ordered structures achieve unprecedented specific electromagnetic interference shielding efficiency

*Peng Chen[1], Shibo He[1], Tianyou Wang[1], Chencan Wang[1], Junru Tao[1], Yiwen Li[1,]**

[1]College of Polymer Science and Engineering, National Key Laboratory of Advanced Polymer Materials, Sichuan University, Chengdu 610065, China.

E-mail: ywli@scu.edu.cn (Y.L.), Tel: +86 028-85401066

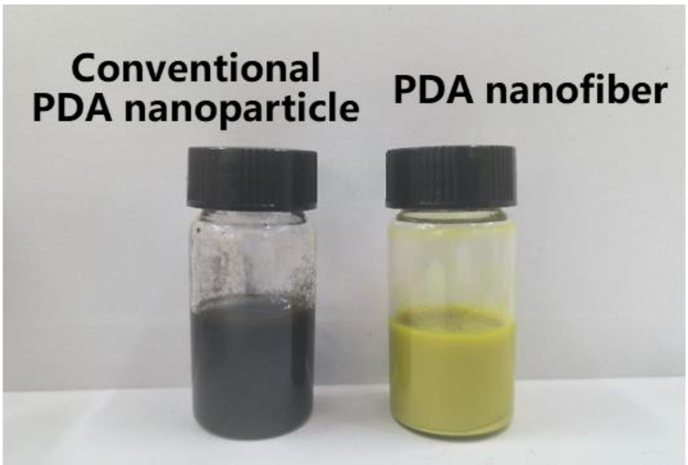

Figure S1. Optical photographs of PDA nanoparticles and nanofibers.

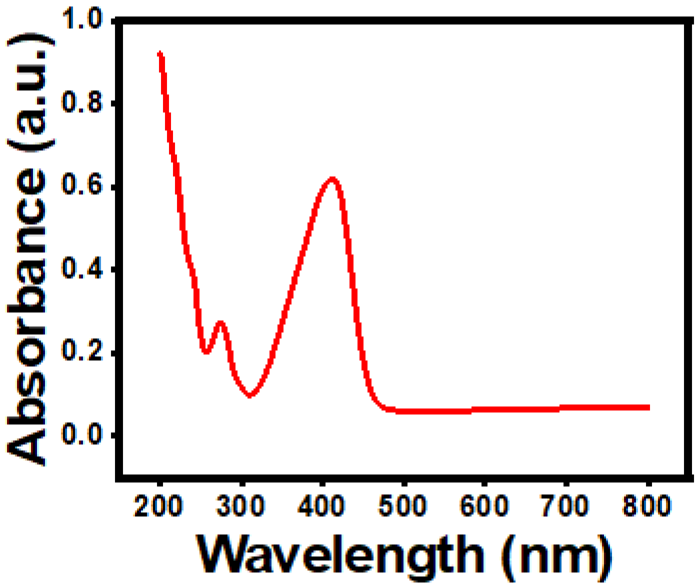

Figure S2. UV–Vis spectrum of the PDA nanofibers.

Scanning electron microscopy (SEM) images showed the morphologies of resulting PDAs (Figure S3). It was observed that the PDAs with indole and 5,6-dihydroxyl indole retained the morphology of nanoparticles, while the PDAs with 5-hydroxylindole showed the morphology of nanofibers, which indicated the possibility of oriented assembly behavior.

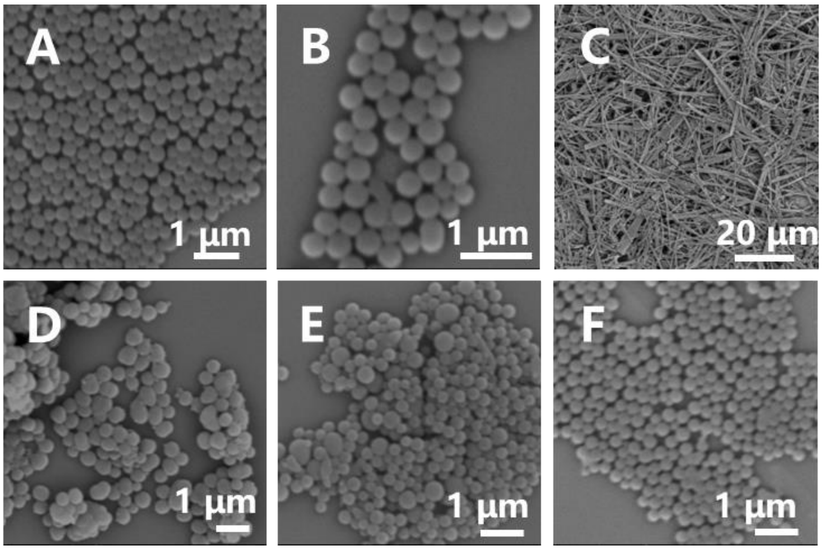

Figure S3. SEM image of PDA (A) nanoparticles, (B) nanoparticles with indole (C) nanofibers with 5-hydroxyindole (D)nanoparticles with 4-hydroxyindole (E) nanoparticlse with 6-hydroxyindole and (F) nanoparticles with 5,6-Dihydroxyindole in the same method.

By controlling the ratio of 5-hydroxyindole, the length-diameter ratio of PDA nanofibers decreased with the increase of indole content, but no fiber was formed when the input was less than 0.05 mass ratio(Figure. S4). Meanwhile, by controlling the ratio of 5-hydroxyindole to dopamine and the amount of alkali, the morphology of the PDA nanofibers showed regular changes, and the length-diameter ratio of the PDA nanofibers was larger with larger amount of alkali and smaller proportion and the length varied from several microns to over 100 microns at 5-hydroxyindole additive concentrations of 0.1 with 0.017 vol% ammonia liquor(Figure. S5).

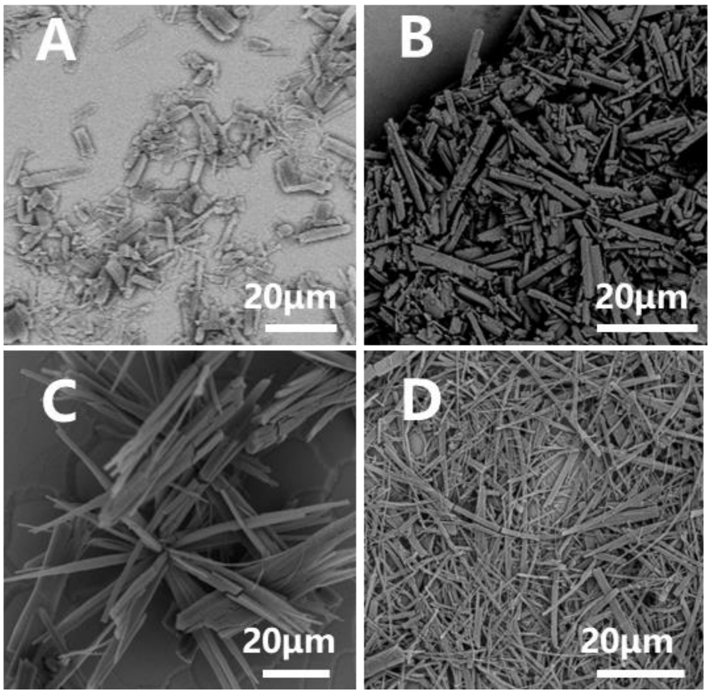

Figure S4. SEM image of nanofibers with different ratios of dopamione:5-hydroxyindole (A)1:1, (B)3:1, (C) 6:1 and (D) 9:1.

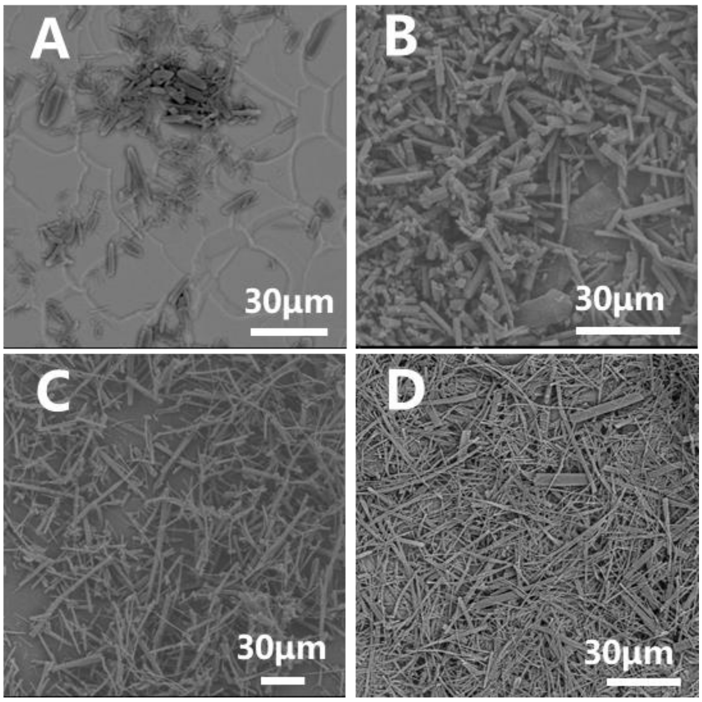

Figure S5. SEM image of nanofibers with different concentrations of ammonia liquor. (A) 0.083 vol% (B) 0.068 vol% (C)0.034 vol% (D) 0.017 vol%.

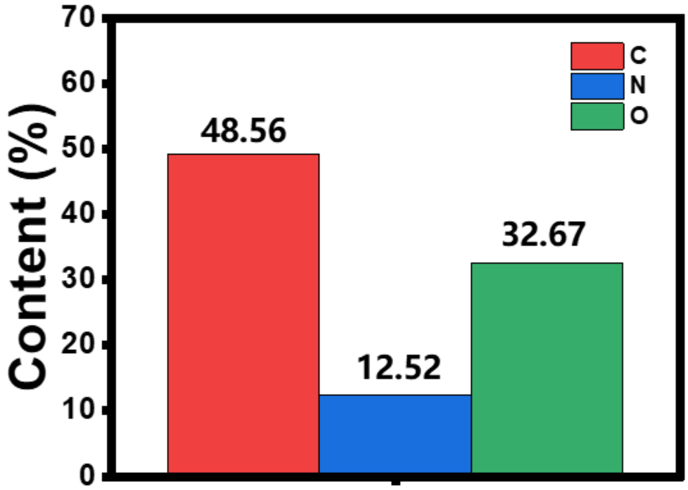

Figure S6. C, N, O element ratio of PDA nanofibers by element analyzer.

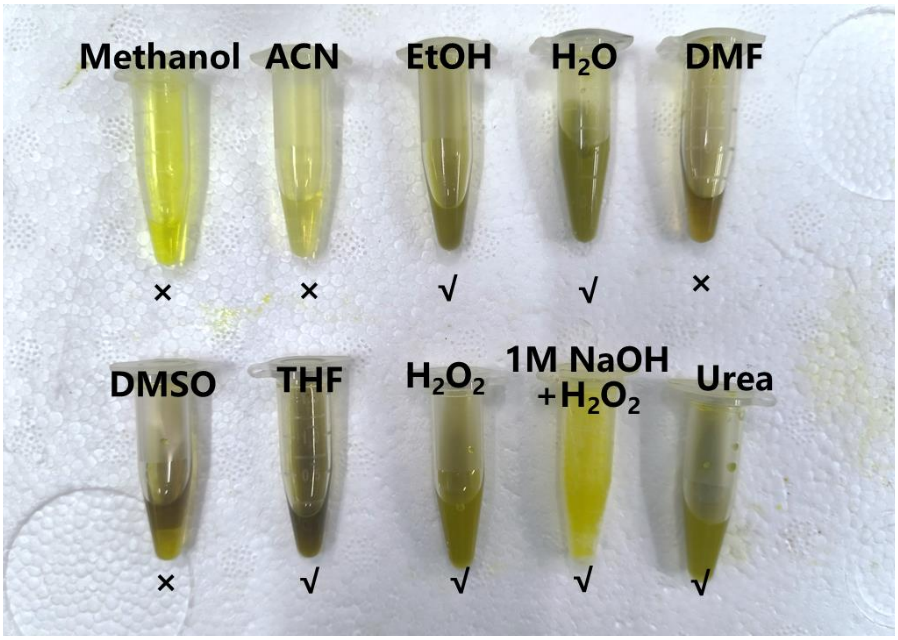

Figure S7. (a) Optical photograph of PDA nanofibers in different solvents. " √ " stands for stability, while "×" stands for degradation.

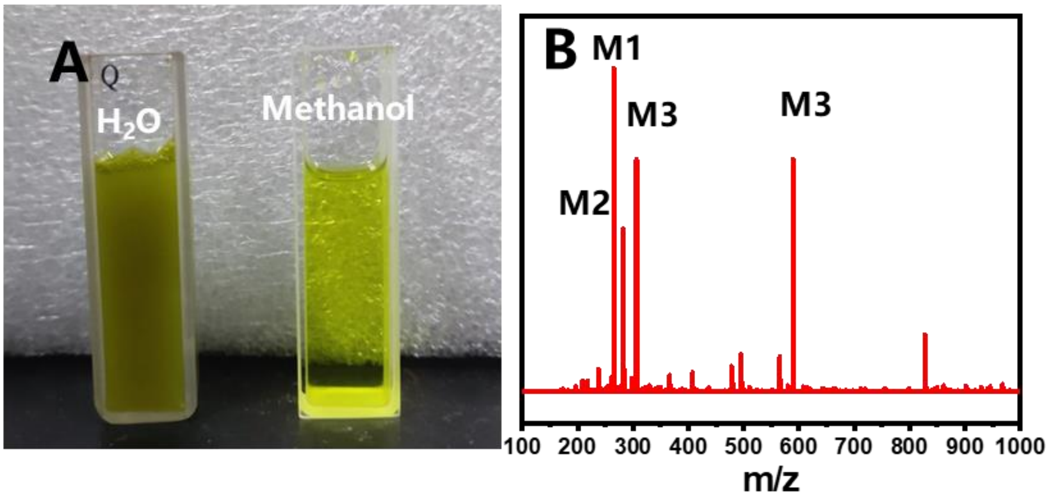

Figure S8. (A) Optical photograph of PDA nanofibers in methanol solution and water solution. (B) Electrospray Ionization Mass Spectrometry of nanofibers methanol solution.

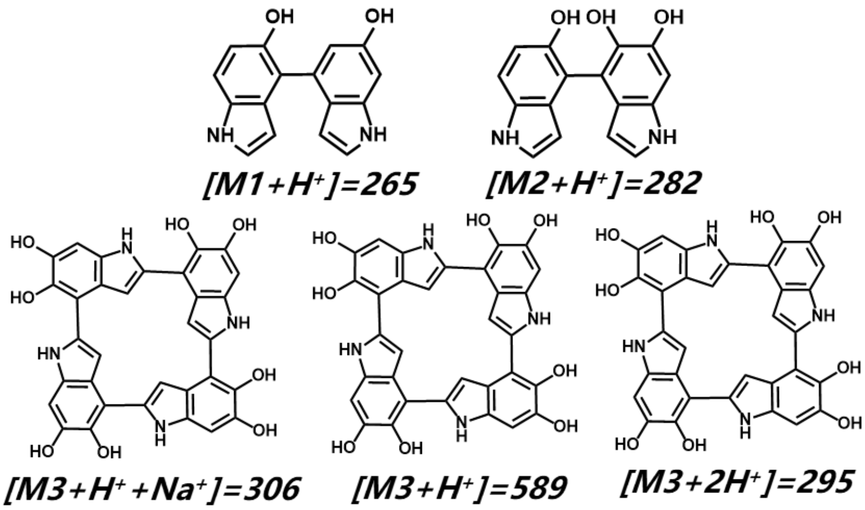

Figure S9. Proposed intermediate molecular structures assigned to main peaks in Fig. S6.

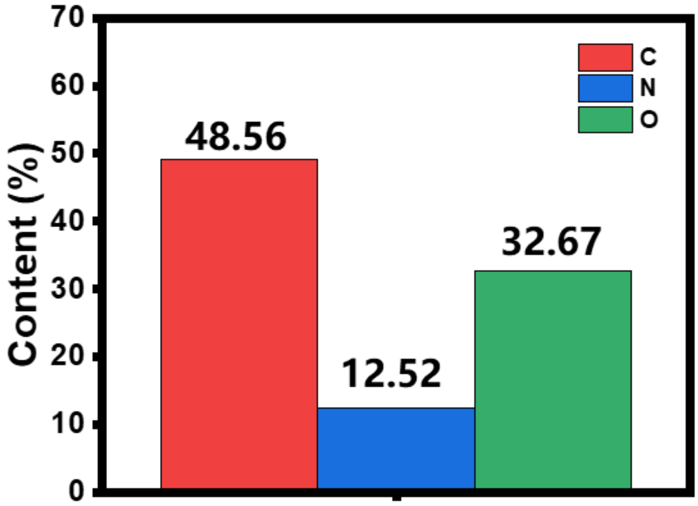

Figure S10. C, N, O element ratio of PDA nanofibers by element analyzer.

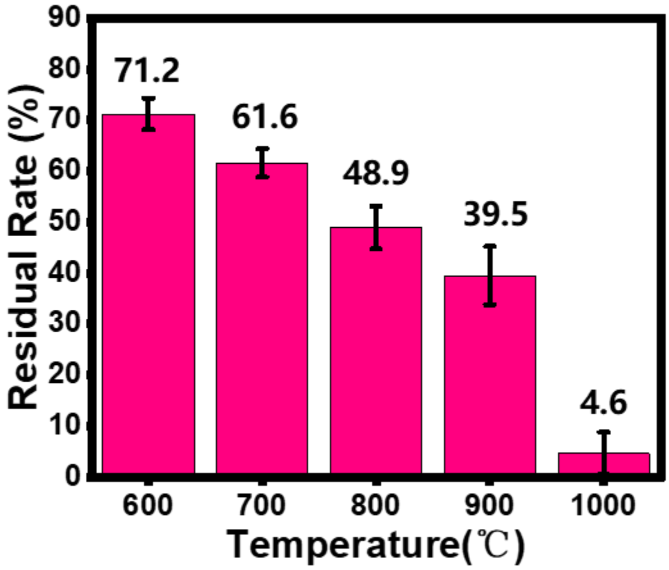

Figure S11. Residual rate of NFAGs at different temperatures.

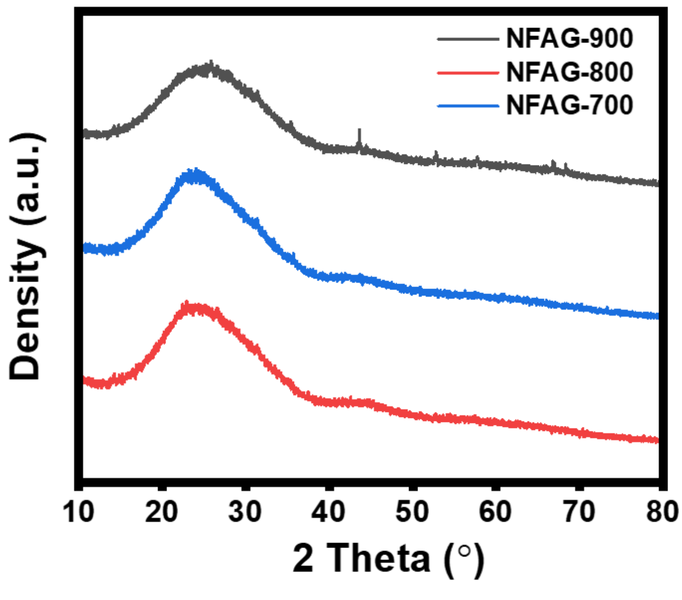

Figure S12. XRD patterns of NFAG-700, NFAG-800, NFAG-900.

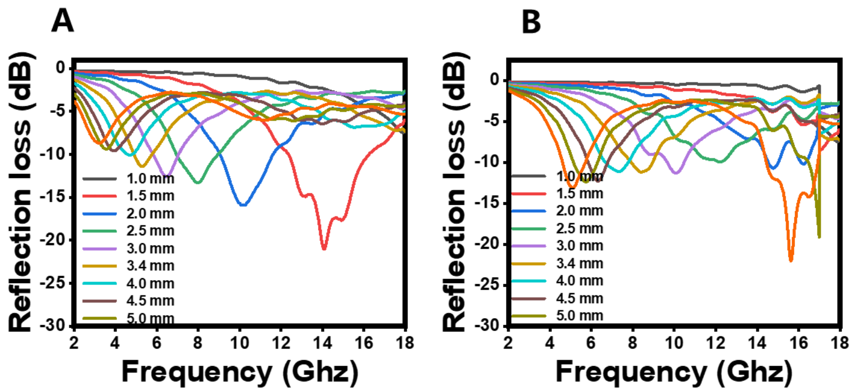

Figure S13. RL values of NFAG-900 with (A) 90% paraffin wax, (B) 70% paraffin wax.

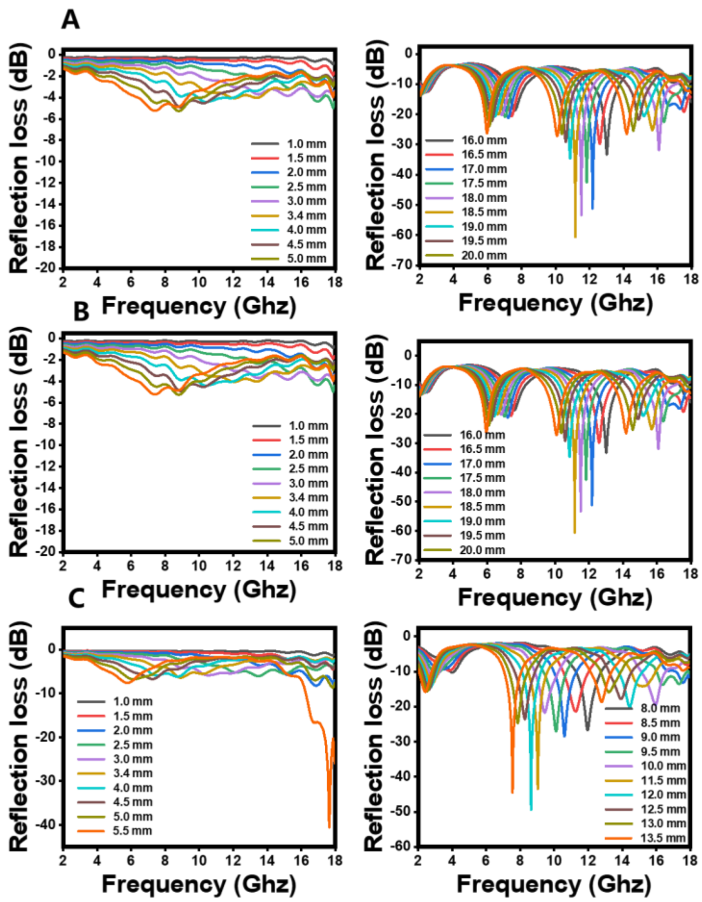

Figure S14. RL values of (A)NFAG-600, (B)NFAG-700, (C)NFAG-800 with 20% paraffin wax.

Generally, the key indicators used to evaluate absorbing materials include EAB and RL_{min}. The real part of complex permittivity and permeability (ε 'and μ', respectively) represented the ability to store electromagnetic energy, while the imaginary part (ε "and μ", respectively) represents the ability to consume electromagnetic energy.

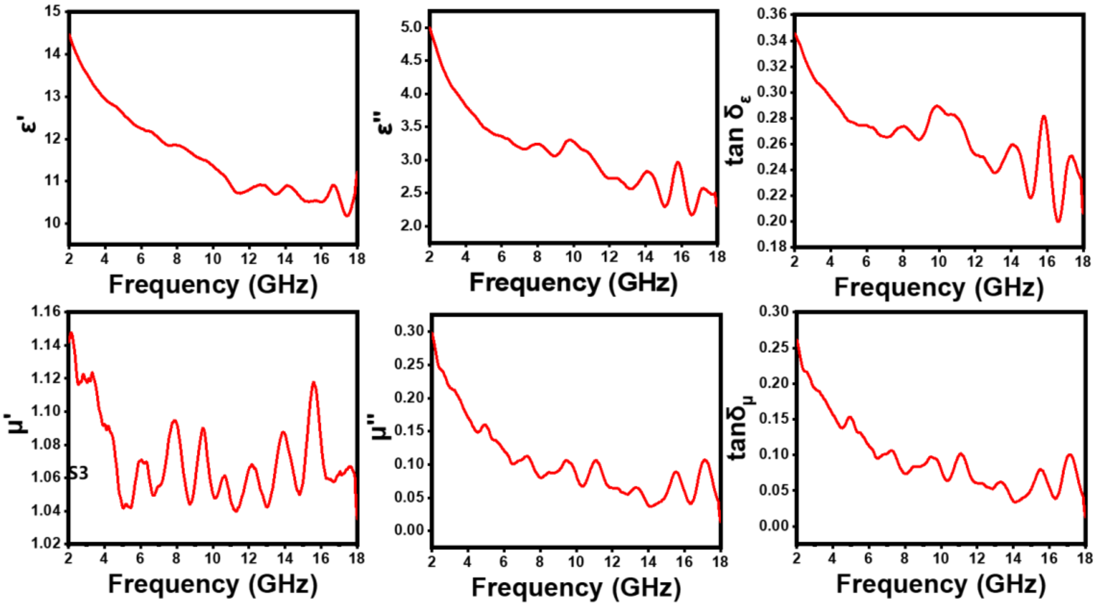

Figure S15. The relevant electromagnetic parameters of NFAG-900.

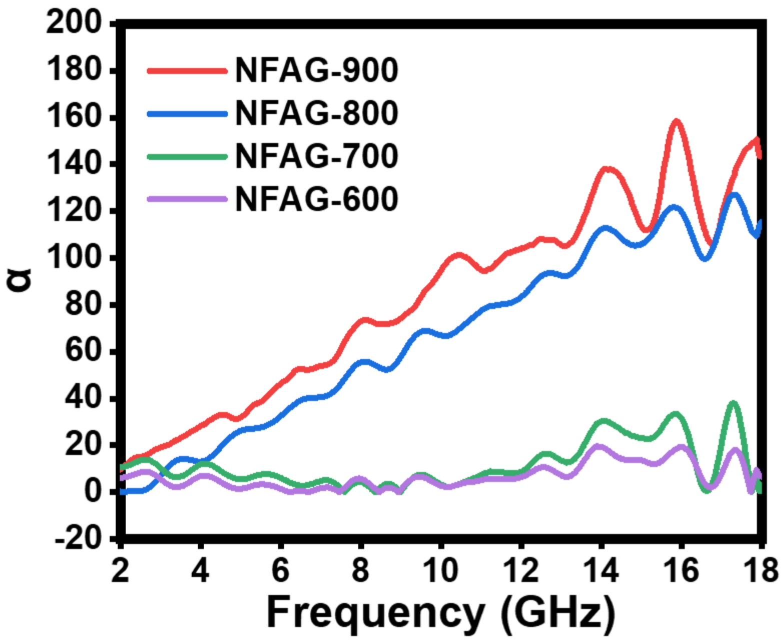

Figure S16. The attenuation constant of NFAGs.

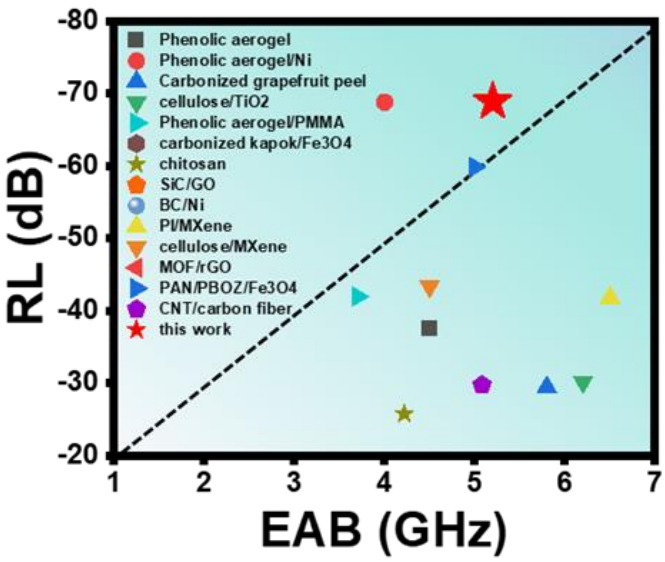

Figure S17 Comparison of RL and EAB of typical reported carbon aerogels for more related work.

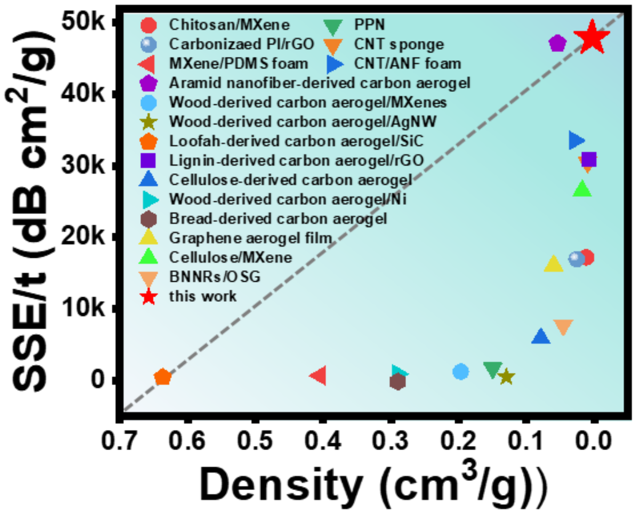

Figure S18. Comparison of SSE/t of typical reported carbon aerogels as a function of density for more related work.

Table S1. Comparison of RL and EAB of typical reported carbon aerogels.

Materials	RL (dB)	EAB (GHz)	Reference
Phenolic aerogel	**-37.5**	4.5	[1]
Phenolic aerogel/Ni	-68.8	4	[2]
Carbonized grapefruit peel	-29.5	5.8	[3]
cellulose/TiO_2	-30.2	6.2	[4]
Phenolic aerogel/PMMA	-42	3.7	[5]
carbonized kapok/Fe_3O_4	-17.3	2.1	[6]
chitosan	-25.8	4.22	[7]

SiC/GO	−47.3	4.7	8
BC/Ni	−55.5	5.35	9
PI/MXene	-41.8	6.5	10
cellulose/MXene	-43.4	4.5	11
MOF/rGO	− 58.1	6.48	12
PAN/PBOZ/Fe_3O_4	-59.85	5	13
CNT/carbon fiber	29.8	5.08	14
This work	**-68.9**	**5.25**	

Table S2. Comparison of SSE/t of typical reported carbon aerogels as a function of density.

Materials	**SSE/t (dB cm^2/g)**	**Density (cm^3/g)**	**Reference**
Chitosan/MXene	17184	0.0119	15
PPN	1700	0.15	16
Wood-derived carbon aerogel/Ni	882.9	0.29	17
Bread-derived carbon	-180.5	0.29	18

aerogel			
Wood-derived carbon aerogel/AgNW	465.1	0.13	[19]
Loofah-derived carbon aerogel/SiC	421.4	0.637	[20]
Carbonizaed PI/rGO	16938.8	0.026	[21]
Cellulose-derived carbon aerogel	5892.4	0.079	[22]
Graphene aerogel film	16071.4	0.06	[23]
CNT sponge	30444.4	0.01	[24]
MXene/PDMS foam	665.4	0.405	[25]
CNT/ANF foam	33528.3	0.029	[26]
Aramid nanofiber-derived carbon aerogel	47122.6	0.0544	[27]
Lignin-derived carbon aerogel/rGO	30750	0.008	[28]
Wood-derived carbon aerogel/MXenes	1206	0.197	[29]

Cellulose/MXene	26500	0.018	[30]
BNNRs/OSG	7700	0.0458	[31]
This work	**40785.9**	**0.00311**	

References：

1. K. J. Wang, Z. W. Ye, X. Q. Li and J. N. Yang, *Materials Chemistry and Physics*, 2022, **278**, 125718.
2. H. B. Zhao, Z. B. Fu, X. Y. Liu, X. C. Zhou, H. B. Chen, M. L. Zhong and C. Y. Wang, *Industrial & Engineering Chemistry Research*, 2018, **57**, 202-211.
3. W. H. Gu, J. Q. Sheng, Q. Q. Huang, G. H. Wang, J. B. Chen and G. B. Ji, *Nano-Micro Letters*, 2021, **13**, 10.1007/s40820-40021-00635-40821.
4. Y. Y. Wang, J. L. Zhu, N. Li, J. F. Shi, J. H. Tang, D. X. Yan and Z. M. Li, *Nano Research*, 2022, **15**, 7723-7730.
5. A. A. Mahani, S. Motahari and V. Nayyeri, *Rsc Advances*, 2018, **8**, 10855-10864.
6. S. K. Song, H. Ai, W. T. Zhu, L. D. Lv, R. Feng and L. J. Dong, *Composites Part B-Engineering*, 2021, **226**, 109330.
7. X. T. Chen, M. Zhou, Y. Zhao, W. H. Gu, Y. Wu, S. L. Tang and G. B. Ji, *Green Chemistry*, 2022, **24**, 5280-5290.
8. Y. Jiang, Y. Chen, Y. J. Liu and G. X. Sui, *Chemical Engineering Journal*, 2018, **337**, 522-531.
9. L. L. Liang, Z. Q. Zhang, F. Song, W. Zhang, H. Li, J. J. Gu, Q. L. Liu and D. Zhang, *Carbon*, 2020, **162**, 283-291.
10. Y. Dai, X. Y. Wu, Z. S. Liu, H. B. Zhang and Z. Z. Yu, *Composites Part B-Engineering*, 2020, **200**, 108263.
11. Y. Jiang, X. Xie, Y. Chen, Y. J. Liu, R. Yang and G. X. Sui, *Journal of Materials Chemistry C*, 2018, **6**, 8679-8687.
12. X. G. Huang, J. W. Wei, Y. K. Zhang, B. B. Qian, Q. Jia, J. Liu, X. J. Zhao and G. F. Shao, *Nano-Micro Letters*, 2022, **14**, 10.1007/s40820-40022-00851-40823.
13. Y. Li, X. F. Liu, X. Y. Nie, W. W. Yang, Y. D. Wang, R. H. Yu and J. L. Shui, *Advanced Functional Materials*, 2019, **29**, 201807624.
14. Y. Cheng, H. Q. Zhao, H. L. Lv, T. F. Shi, G. B. Ji and Y. L. Hou, *Advanced Electronic Materials*, 2020, **6**, 201900796.

15. S. Q. Wu, D. M. Chen, W. B. Han, Y. S. Xie, G. D. Zhao, S. Dong, M. Y. Tan, H. Huang, S. B. Xu, G. Q. Chen, Y. Cheng and X. H. Zhang, *Chemical Engineering Journal*, 2022, **446**.
16. L. Y. Zhang, M. Liu, S. Roy, E. K. Chu, K. Y. See and X. Hu, *Acs Applied Materials & Interfaces*, 2016, **8**, 7422-7430.
17. Y. Zheng, Y. J. Song, T. Gao, S. Y. Yan, H. H. Hu, F. Cao, Y. P. Duan and X. F. Zhang, *Acs Applied Materials & Interfaces*, 2020, **12**, 40802-40814.
18. Y. Yuan, Y. J. Ding, C. H. Wang, F. Xu, Z. S. Lin, Y. Y. Qin, Y. Li, M. L. Yang, X. D. He, Q. Y. Peng and Y. B. Li, *Acs Applied Materials & Interfaces*, 2016, **8**, 16852-16861.
19. Y. Yuan, X. X. Sun, M. L. Yang, F. Xu, Z. S. Lin, X. Zhao, Y. J. Ding, J. J. Li, W. L. Yin, Q. Y. Peng, X. D. He and Y. B. Li, *Acs Applied Materials & Interfaces*, 2017, **9**, 21371-21381.
20. S. T. Li, D. Y. Liu, W. C. Li and G. X. Sui, *Acs Sustainable Chemistry & Engineering*, 2020, **8**, 435-444.
21. J. Liu, Y. F. Liu, H. B. Zhang, Y. Dai, Z. S. Liu and Z. Z. Yu, *Carbon*, 2018, **132**, 95-103.
22. Z. H. Zhou, Y. Liang, H. D. Huang, L. Li, B. Yang, M. Z. Li, D. X. Yan, J. Lei and Z. M. Li, *Carbon*, 2019, **152**, 316-324.
23. J. B. Xi, Y. L. Li, E. Z. Zhou, Y. J. Liu, W. W. Gao, Y. Guo, J. Ying, Z. C. Chen, G. G. Chen and C. Gao, *Carbon*, 2018, **135**, 44-51.
24. D. W. Lu, Z. C. Mo, B. H. Liang, L. L. Yang, Z. F. He, H. Zhu, Z. K. Tang and X. C. Gui, *Carbon*, 2018, **133**, 457-463.
25. X. Y. Wu, B. Y. Han, H. B. Zhang, X. Xie, T. X. Tu, Y. Zhang, Y. Dai, R. Yang and Z. Z. Yu, *Chemical Engineering Journal*, 2020, **381**.
26. P. Y. Hu, J. Lyu, C. Fu, W. B. Gong, J. H. Liao, W. B. Lu, Y. P. Chen and X. T. Zhang, *Acs Nano*, 2020, **14**, 688-697.
27. B. Zhou, G. J. Han, Z. Zhang, Z. Y. Li, Y. Z. Feng, J. M. Ma, C. T. Liu and C. Y. Shen, *Carbon*, 2021, **184**, 562-570.
28. Z. H. Zeng, C. X. Wang, Y. F. Zhang, P. Y. Wang, S. I. S. Shahabadi, Y. M. Pei, M. J. Chen and X. H. Lu, *Acs Applied Materials & Interfaces*, 2018, **10**, 8205-8213.
29. C. B. Liang, H. Qiu, P. Song, X. T. Shi, J. Kong and J. W. Gu, *Science Bulletin*, 2020, **65**, 616-622.
30. N. Wu, Y. F. Yang, C. X. Wang, Q. L. Wu, F. Pan, R. A. Zhang, J. R. Liu and Z. H. Zeng, *Advanced Materials*, DOI: 10.1002/adma.202207969, 202207969.
31. L. Feng, P. Wei, Q. Song, J. X. Zhang, Q. G. Fu, X. H. Jia, J. Yang, D. Shao, Y. Li, S. Z. Wang, X. F. Qiang and H. J. Song, *Acs Nano*, 2022, **16**, 17049-17061.